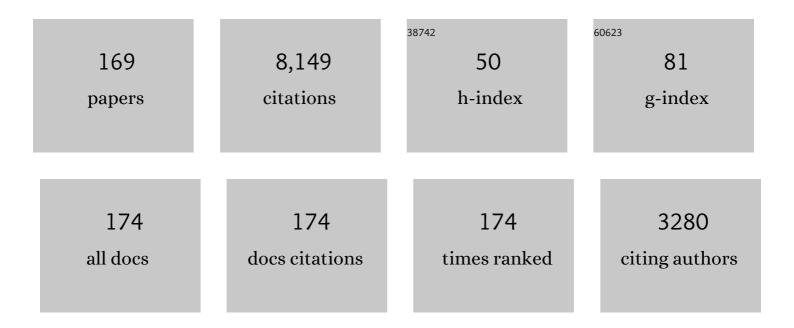
List of Publications by Year in descending order

Source: https://exaly.com/author-pdf/1146428/publications.pdf Version: 2024-02-01



HAIF KODTH

#	Article	IF	CITATIONS
1	The Space Physics Environment Data Analysis System (SPEDAS). Space Science Reviews, 2019, 215, 9.	8.1	332
2	The Global Magnetic Field of Mercury from MESSENGER Orbital Observations. Science, 2011, 333, 1859-1862.	12.6	301
3	The Magnetometer Instrument on MESSENGER. Space Science Reviews, 2007, 131, 417-450.	8.1	254
4	MESSENGER Observations of Magnetic Reconnection in Mercury's Magnetosphere. Science, 2009, 324, 606-610.	12.6	234
5	The Structure of Mercury's Magnetic Field from MESSENGER's First Flyby. Science, 2008, 321, 82-85.	12.6	194
6	Mercury's magnetopause and bow shock from MESSENGER Magnetometer observations. Journal of Geophysical Research: Space Physics, 2013, 118, 2213-2227.	2.4	182
7	Plasma sheet access to geosynchronous orbit. Journal of Geophysical Research, 1999, 104, 25047-25061.	3.3	176
8	MESSENGER Observations of Extreme Loading and Unloading of Mercury's Magnetic Tail. Science, 2010, 329, 665-668.	12.6	172
9	Mercury's Magnetosphere After MESSENGER's First Flyby. Science, 2008, 321, 85-89.	12.6	166
10	Development of large-scale Birkeland currents determined from the Active Magnetosphere and Planetary Electrodynamics Response Experiment. Geophysical Research Letters, 2014, 41, 3017-3025.	4.0	156
11	MESSENGER observations of magnetopause structure and dynamics at Mercury. Journal of Geophysical Research: Space Physics, 2013, 118, 997-1008.	2.4	141
12	Bulk plasma properties at geosynchronous orbit. Journal of Geophysical Research, 2005, 110, .	3.3	135
13	Statistical Birkeland current distributions from magnetic field observations by the Iridium constellation. Annales Geophysicae, 2008, 26, 671-687.	1.6	132
14	Lowâ€degree structure in Mercury's planetary magnetic field. Journal of Geophysical Research, 2012, 117,	3.3	131
15	MESSENGER observations of Mercury's dayside magnetosphere under extreme solar wind conditions. Journal of Geophysical Research: Space Physics, 2014, 119, 8087-8116.	2.4	125
16	Mercury's magnetospheric magnetic field after the first two MESSENGER flybys. Icarus, 2010, 209, 23-39.	2.5	110
17	MESSENGER observations of Mercury's magnetic field structure. Journal of Geophysical Research, 2012, 117, .	3.3	109
18	Overview of Solar Wind–Magnetosphere–Ionosphere–Atmosphere Coupling and the Generation of Magnetospheric Currents. Space Science Reviews, 2017, 206, 547-573.	8.1	105

#	Article	IF	CITATIONS
19	MESSENGER Observations of the Spatial Distribution of Planetary Ions Near Mercury. Science, 2011, 333, 1862-1865.	12.6	102
20	Magnetic flux pileup and plasma depletion in Mercury's subsolar magnetosheath. Journal of Geophysical Research: Space Physics, 2013, 118, 7181-7199.	2.4	96
21	The Magnetic Field of Mercury. Space Science Reviews, 2010, 152, 307-339.	8.1	94
22	Low-altitude magnetic field measurements by MESSENGER reveal Mercury's ancient crustal field. Science, 2015, 348, 892-895.	12.6	89
23	MESSENGER and Mariner 10 flyby observations of magnetotail structure and dynamics at Mercury. Journal of Geophysical Research, 2012, 117, .	3.3	86
24	Observations of Mercury's northern cusp region with MESSENGER's Magnetometer. Geophysical Research Letters, 2012, 39, .	4.0	86
25	Remote and in situ observations of an unusual Earthâ€directed coronal mass ejection from multiple viewpoints. Journal of Geophysical Research, 2012, 117, .	3.3	86
26	MESSENGER observations of a fluxâ€ŧransferâ€event shower at Mercury. Journal of Geophysical Research, 2012, 117, .	3.3	85
27	Distribution and compositional variations of plasma ions in Mercury's space environment: The first three Mercury years of MESSENGER observations. Journal of Geophysical Research: Space Physics, 2013, 118, 1604-1619.	2.4	85
28	Structure and dynamics of Mercury's magnetospheric cusp: MESSENGER measurements of protons and planetary ions. Journal of Geophysical Research: Space Physics, 2014, 119, 6587-6602.	2.4	79
29	MESSENGER observations of the plasma environment near Mercury. Planetary and Space Science, 2011, 59, 2004-2015.	1.7	78
30	Seasonal and diurnal variations in AMPERE observations of the Birkeland currents compared to modeled results. Journal of Geophysical Research: Space Physics, 2016, 121, 4027-4040.	2.4	76
31	Impact of toroidal ULF waves on the outer radiation belt electrons. Journal of Geophysical Research, 2005, 110, .	3.3	72
32	MESSENGER observations of dipolarization events in Mercury's magnetotail. Journal of Geophysical Research, 2012, 117, .	3.3	72
33	MESSENGER observations of flux ropes in Mercury's magnetotail. Planetary and Space Science, 2015, 115, 77-89.	1.7	71
34	MESSENGER orbital observations of largeâ€amplitude Kelvinâ€Helmholtz waves at Mercury's magnetopause. Journal of Geophysical Research, 2012, 117, .	3.3	69
35	Modeling of the magnetosphere of Mercury at the time of the first MESSENGER flyby. Icarus, 2010, 209, 3-10.	2.5	67
36	The detailed spatial structure of fieldâ€aligned currents comprising the substorm current wedge. Journal of Geophysical Research: Space Physics, 2013, 118, 7714-7727.	2.4	63

#	Article	IF	CITATIONS
37	Determination of the properties of Mercury's magnetic field by the MESSENGER mission. Planetary and Space Science, 2004, 52, 733-746.	1.7	61
38	Seasonal and interplanetary magnetic field dependence of the field-aligned currents for both Northern and Southern Hemispheres. Annales Geophysicae, 2009, 27, 1701-1715.	1.6	60
39	Modular model for Mercury's magnetospheric magnetic field confined within the average observed magnetopause. Journal of Geophysical Research: Space Physics, 2015, 120, 4503-4518.	2.4	59
40	Plasma sheet access to the inner magnetosphere. Journal of Geophysical Research, 2001, 106, 5845-5858.	3.3	58
41	Statistical relationship between largeâ€scale upward fieldâ€eligned currents and electron precipitation. Journal of Geophysical Research: Space Physics, 2014, 119, 6715-6731.	2.4	58
42	MESSENGER observations of large flux transfer events at Mercury. Geophysical Research Letters, 2010, 37, .	4.0	57
43	The magnitudes of the regions 1 and 2 Birkeland currents observed by AMPERE and their role in solar windâ€magnetosphereâ€ionosphere coupling. Journal of Geophysical Research: Space Physics, 2014, 119, 9804-9815.	2.4	56
44	MESSENGER: Exploring Mercury's Magnetosphere. Space Science Reviews, 2007, 131, 133-160.	8.1	55
45	MESSENGER observations of Mercury's magnetosphere during northward IMF. Geophysical Research Letters, 2009, 36, .	4.0	55
46	Steadyâ€state fieldâ€aligned currents at Mercury. Geophysical Research Letters, 2014, 41, 7444-7452.	4.0	55
47	Solar wind alpha particles and heavy ions in the inner heliosphere observed with MESSENGER. Journal of Geophysical Research, 2012, 117, .	3.3	54
48	MESSENGER observations of large dayside flux transfer events: Do they drive Mercury's substorm cycle?. Journal of Geophysical Research: Space Physics, 2014, 119, 5613-5623.	2.4	54
49	MESSENGER observations of induced magnetic fields in Mercury's core. Geophysical Research Letters, 2016, 43, 2436-2444.	4.0	51
50	Observations of Kelvinâ€Helmholtz waves along the duskâ€side boundary of Mercury's magnetosphere during MESSENGER's third flyby. Geophysical Research Letters, 2010, 37, .	4.0	50
51	lon kinetic properties in Mercury's preâ€midnight plasma sheet. Geophysical Research Letters, 2014, 41, 5740-5747.	4.0	50
52	MESSENGER observations of magnetospheric substorm activity in Mercury's near magnetotail. Geophysical Research Letters, 2015, 42, 3692-3699.	4.0	50
53	A superposed epoch analysis of the regions 1 and 2 Birkeland currents observed by AMPERE during substorms. Journal of Geophysical Research: Space Physics, 2014, 119, 9834-9846.	2.4	48
54	Solar wind forcing at Mercury: WSAâ€ENLIL model results. Journal of Geophysical Research: Space Physics, 2013, 118, 45-57.	2.4	46

#	Article	IF	CITATIONS
55	Global ionospheric and thermospheric response to the 5 April 2010 geomagnetic storm: An integrated dataâ€model investigation. Journal of Geophysical Research: Space Physics, 2014, 119, 10,358.	2.4	46
56	Plasma distribution in Mercury's magnetosphere derived from MESSENGER Magnetometer and Fast Imaging Plasma Spectrometer observations. Journal of Geophysical Research: Space Physics, 2014, 119, 2917-2932.	2.4	46
57	Miniature atomic scalar magnetometer for space based on the rubidium isotope ⁸⁷ Rb. Journal of Geophysical Research: Space Physics, 2016, 121, 7870-7880.	2.4	46
58	Statistical analysis of the dependence of large-scale Birkeland currents on solar wind parameters. Annales Geophysicae, 2010, 28, 515-530.	1.6	45
59	Comprehensive particle and field observations of magnetic storms at different local times from the CRRES spacecraft. Journal of Geophysical Research, 2000, 105, 18729-18740.	3.3	41
60	Modeling Mercury's internal magnetic field with smooth inversions. Earth and Planetary Science Letters, 2009, 285, 328-339.	4.4	41
61	Global Empirical Picture of Magnetospheric Substorms Inferred From Multimission Magnetometer Data. Journal of Geophysical Research: Space Physics, 2019, 124, 1085-1110.	2.4	41
62	Cluster observations in the inner magnetosphere during the 18 April 2002 sawtooth event: Dipolarization and injection at <i>r</i> = 4.6 <i>R</i> _{<i>E</i>} . Journal of Geophysical Research, 2007, 112, .	3.3	40
63	Quasi-trapped ion and electron populations at Mercury. Geophysical Research Letters, 2011, 38, n/a-n/a.	4.0	40
64	Upstream ultraâ€low frequency waves in Mercury's foreshock region: MESSENGER magnetic field observations. Journal of Geophysical Research: Space Physics, 2013, 118, 2809-2823.	2.4	40
65	MESSENGER observations of multiscale Kelvinâ€Helmholtz vortices at Mercury. Journal of Geophysical Research: Space Physics, 2015, 120, 4354-4368.	2.4	40
66	MESSENGER X-ray observations of magnetosphere–surface interaction on the nightside of Mercury. Planetary and Space Science, 2016, 125, 72-79.	1.7	40
67	Storm time dawn-dusk asymmetry of the large-scale Birkeland currents. Journal of Geophysical Research, 2005, 110, .	3.3	39
68	Kinetic-scale magnetic turbulence and finite Larmor radius effects at Mercury. Journal of Geophysical Research, 2011, 116, n/a-n/a.	3.3	39
69	Survey of coherent â^¼1 Hz waves in Mercury's inner magnetosphere from MESSENGER observations. Journal of Geophysical Research, 2012, 117, .	3.3	39
70	A magnetic disturbance index for Mercury's magnetic field derived from MESSENGER Magnetometer data. Geochemistry, Geophysics, Geosystems, 2013, 14, 3875-3886.	2.5	39
71	Mercury's surface magnetic field determined from protonâ€reflection magnetometry. Geophysical Research Letters, 2014, 41, 4463-4470.	4.0	39
72	Empirical modeling of a CIRâ€driven magnetic storm. Journal of Geophysical Research, 2010, 115, .	3.3	38

#	Article	IF	CITATIONS
73	Plasma pressure in Mercury's equatorial magnetosphere derived from MESSENGER Magnetometer observations. Geophysical Research Letters, 2011, 38, n/a-n/a.	4.0	38
74	Principal component analysis of Birkeland currents determined by the Active Magnetosphere and Planetary Electrodynamics Response Experiment. Journal of Geophysical Research: Space Physics, 2015, 120, 10,415.	2.4	38
75	MESSENGER and Venus Express observations of the solar wind interaction with Venus. Geophysical Research Letters, 2009, 36, .	4.0	37
76	The Kelvin–Helmholtz instability at Mercury: An assessment. Planetary and Space Science, 2010, 58, 1434-1441.	1.7	36
77	Comprehensive survey of energetic electron events in Mercury's magnetosphere with data from the MESSENGER Gammaâ€Ray and Neutron Spectrometer. Journal of Geophysical Research: Space Physics, 2015, 120, 2851-2876.	2.4	36
78	Intercomparison of ionospheric electrodynamics from the Iridium constellation with global MHD simulations. Journal of Geophysical Research, 2004, 109, .	3.3	35
79	The interplanetary magnetic field environment at Mercury's orbit. Planetary and Space Science, 2011, 59, 2075-2085.	1.7	35
80	MESSENGER Observations of Transient Bursts of Energetic Electrons in Mercury's Magnetosphere. Science, 2011, 333, 1865-1868.	12.6	35
81	MESSENGER observations of suprathermal electrons in Mercury's magnetosphere. Geophysical Research Letters, 2016, 43, 550-555.	4.0	35
82	Comparison of predictive estimates of high″atitude electrodynamics with observations of globalâ€scale Birkeland currents. Space Weather, 2017, 15, 352-373.	3.7	35
83	Pressure balance inconsistency exhibited in a statistical model of magnetospheric plasma. Journal of Geophysical Research, 2003, 108, .	3.3	34
84	Contribution of convective transport to stormtime ring current electron injection. Journal of Geophysical Research, 2003, 108, .	3.3	34
85	The dayside magnetospheric boundary layer at Mercury. Planetary and Space Science, 2011, 59, 2037-2050.	1.7	33
86	Empirical relationship between electron precipitation and farâ€ultraviolet auroral emissions from DMSP observations. Journal of Geophysical Research: Space Physics, 2013, 118, 1203-1209.	2.4	33
87	Comparison of magnetic perturbation data from LEO satellite constellations: Statistics of DMSP and AMPERE. Space Weather, 2014, 12, 2-23.	3.7	33
88	High-latitude electromagnetic and particle energy flux during an event with sustained strongly northward IMF. Annales Geophysicae, 2005, 23, 1295-1310.	1.6	31
89	Global evolution of Birkeland currents on 10 min timescales: MHD simulations and observations. Journal of Geophysical Research: Space Physics, 2013, 118, 4977-4997.	2.4	31
90	Intense energetic electron flux enhancements in Mercury's magnetosphere: An integrated view with highâ€resolution observations from MESSENGER. Journal of Geophysical Research: Space Physics, 2016, 121, 2171-2184.	2.4	31

#	Article	IF	CITATIONS
91	Electron transport and precipitation at Mercury during the MESSENGER flybys: Implications for electron-stimulated desorption. Planetary and Space Science, 2011, 59, 2026-2036.	1.7	30
92	A Dynamic Model of Mercury's Magnetospheric Magnetic Field. Geophysical Research Letters, 2017, 44, 10147-10154.	4.0	30
93	Empirical reconstruction of storm time steady magnetospheric convection events. Journal of Geophysical Research: Space Physics, 2013, 118, 6434-6456.	2.4	29
94	First observations of Mercury's plasma mantle by MESSENGER. Geophysical Research Letters, 2015, 42, 9666-9675.	4.0	29
95	MESSENGER observations of cusp plasma filaments at Mercury. Journal of Geophysical Research: Space Physics, 2016, 121, 8260-8285.	2.4	29
96	The space environment of Mercury at the times of the second and third MESSENGER flybys. Planetary and Space Science, 2011, 59, 2066-2074.	1.7	28
97	Spatial distribution and spectral characteristics of energetic electrons in Mercury's magnetosphere. Journal of Geophysical Research, 2012, 117, .	3.3	28
98	Science Data Products for AMPERE. , 2020, , 141-165.		28
99	Plasma sheet access to geosynchronous orbit: Generalization to numerical global field models. Journal of Geophysical Research, 2001, 106, 29655-29667.	3.3	27
100	Comparison of large-scale Birkeland currents determined from Iridium and SuperDARN data. Annales Geophysicae, 2006, 24, 941-959.	1.6	27
101	Narrowâ€band ultraâ€lowâ€frequency wave observations by MESSENGER during its January 2008 flyby through Mercury's magnetosphere. Geophysical Research Letters, 2009, 36, .	4.0	26
102	Cyclic reformation of a quasiâ€parallel bow shock at Mercury: MESSENGER observations. Journal of Geophysical Research: Space Physics, 2013, 118, 6457-6464.	2.4	25
103	Upper cutoff energy of the electron plasma sheet as a measure of magnetospheric convection strength. Journal of Geophysical Research, 2002, 107, SMP 25-1.	3.3	24
104	Seasonal dependence of localized, high-latitude dayside aurora (HiLDA). Journal of Geophysical Research, 2004, 109, .	3.3	24
105	Reconstruction of propagating Kelvin–Helmholtz vortices at Mercury's magnetopause. Planetary and Space Science, 2011, 59, 2051-2057.	1.7	24
106	Reduction in fieldâ€aligned currents preceding and local to auroral substorm onset. Geophysical Research Letters, 2012, 39, .	4.0	24
107	Statistical study of ICME effects on Mercury's magnetospheric boundaries and northern cusp region from MESSENGER. Journal of Geophysical Research: Space Physics, 2017, 122, 4960-4975.	2.4	24
108	Characteristics of the plasma distribution in Mercury's equatorial magnetosphere derived from MESSENGER Magnetometer observations. Journal of Geophysical Research, 2012, 117, .	3.3	23

#	Article	IF	CITATIONS
109	Constraints on the secular variation of Mercury's magnetic field from the combined analysis of MESSENGER and Mariner 10 data. Geophysical Research Letters, 2014, 41, 6627-6634.	4.0	23
110	Mercury's internal magnetic field: Constraints on large- and small-scale fields of crustal origin. Earth and Planetary Science Letters, 2009, 285, 340-346.	4.4	22
111	Active current sheets and candidate hot flow anomalies upstream of Mercury's bow shock. Journal of Geophysical Research: Space Physics, 2014, 119, 853-876.	2.4	22
112	Temporal and Spatial Development of Global Birkeland Currents. Journal of Geophysical Research: Space Physics, 2018, 123, 4785-4808.	2.4	22
113	Technique: Large-scale ionospheric conductance estimated from combined satellite and ground-based electromagnetic data. Journal of Geophysical Research, 2007, 112, n/a-n/a.	3.3	21
114	Comparison of the observed dependence of large-scale Birkeland currents on solar wind parameters with that obtained from global simulations. Annales Geophysicae, 2011, 29, 1809-1826.	1.6	21
115	MESSENGER survey of in situ low frequency wave storms between 0.3 and 0.7 AU. Journal of Geophysical Research: Space Physics, 2015, 120, 10,207.	2.4	21
116	On the formation and origin of substorm growth phase/onset auroral arcs inferred from conjugate spaceâ€ground observations. Journal of Geophysical Research: Space Physics, 2015, 120, 8707-8722.	2.4	21
117	Interpreting ~1 Hz magnetic compressional waves in Mercury's inner magnetosphere in terms of propagating ionâ€Bernstein waves. Journal of Geophysical Research: Space Physics, 2015, 120, 4213-4228.	2.4	21
118	Auroral Current and Electrodynamics Structure (ACES) observations of ionospheric feedback in the Alfvén resonator and model responses. Journal of Geophysical Research: Space Physics, 2013, 118, 3288-3296.	2.4	19
119	Highâ€latitude ionosphere convection and Birkeland current response for the 15 May 2005 magnetic storm recovery phase. Journal of Geophysical Research, 2008, 113, .	3.3	18
120	Comparison of Birkeland current observations during two magnetic cloud events with MHD simulations. Annales Geophysicae, 2008, 26, 499-516.	1.6	17
121	Comparison of ultra″owâ€frequency waves at Mercury under northward and southward IMF. Geophysical Research Letters, 2009, 36, .	4.0	17
122	A comparison of magnetic overshoots at the bow shocks of Mercury and Saturn. Journal of Geophysical Research: Space Physics, 2013, 118, 4381-4390.	2.4	17
123	Electric currents of a substorm current wedge on 24 February 2010. Geophysical Research Letters, 2014, 41, 4449-4455.	4.0	17
124	Saturation of global field aligned currents observed during storms by the Iridium satellite constellation. Journal of Atmospheric and Solar-Terrestrial Physics, 2007, 69, 166-169.	1.6	16
125	Inductive electric fields in the inner magnetosphere during geomagnetically active periods. Journal of Geophysical Research, 2010, 115, .	3.3	16
126	Improving solar wind modeling at Mercury: Incorporating transient solar phenomena into the WSAâ€ENLIL model with the Cone extension. Journal of Geophysical Research: Space Physics, 2015, 120, 5667-5685.	2.4	16

#	Article	IF	CITATIONS
127	MESSENGER observations of solar energetic electrons within Mercury's magnetosphere. Journal of Geophysical Research: Space Physics, 2015, 120, 8559-8571.	2.4	16
128	Filamentary field-aligned currents at the polar cap region during northward interplanetary magnetic field derived with the Swarm constellation. Annales Geophysicae, 2016, 34, 901-915.	1.6	16
129	Timescales of Dayside and Nightside Fieldâ€Aligned Current Response to Changes in Solar Windâ€Magnetosphere Coupling. Journal of Geophysical Research: Space Physics, 2018, 123, 7307-7319.	2.4	16
130	Statistical Relations Between Auroral Electrical Conductances and Fieldâ€Aligned Currents at High Latitudes. Journal of Geophysical Research: Space Physics, 2020, 125, e2020JA028008.	2.4	16
131	Event study combining magnetospheric and ionospheric perspectives of the substorm current wedge modeling. Journal of Geophysical Research: Space Physics, 2014, 119, 9714-9728.	2.4	15
132	Phase-Synchronization, Energy Cascade, and Intermittency in Solar-Wind Turbulence. Physical Review Letters, 2012, 109, 245004.	7.8	14
133	Intense solar nearâ€relativistic electron events at 0.3 AU. Journal of Geophysical Research: Space Physics, 2013, 118, 63-73.	2.4	13
134	Conditions governing localized high-latitude dayside aurora. Geophysical Research Letters, 2004, 31, .	4.0	12
135	The initial temporal evolution of a feedback dynamo for Mercury. Geophysical and Astrophysical Fluid Dynamics, 2010, 104, 419-429.	1.2	12
136	Mercury's Internal Magnetic Field. , 2018, , 114-143.		12
137	Particle tomography of the inner magnetosphere. Journal of Geophysical Research, 2002, 107, SMP 5-1.	3.3	11
138	Global observations of electromagnetic and particle energy flux for an event during northern winter with southward interplanetary magnetic field. Annales Geophysicae, 2008, 26, 1415-1430.	1.6	11
139	A statistical survey of ultralowâ€frequency wave power and polarization in the Hermean magnetosphere. Journal of Geophysical Research: Space Physics, 2016, 121, 8755-8772.	2.4	11
140	Empirical Modeling of Extreme Events: Storm-Time Geomagnetic Field, Electric Current, and Pressure Distributions. , 2018, , 259-279.		11
141	A global MHD simulation of an event with a quasi-steady northward IMF component. Annales Geophysicae, 2007, 25, 1345-1358.	1.6	10
142	Fieldâ€aligned current reconfiguration and magnetospheric response to an impulse in the interplanetary magnetic field <i>B</i> _Y component. Geophysical Research Letters, 2013, 40, 2489-2494.	4.0	10
143	Electrodynamic context of magnetopause dynamics observed by magnetospheric multiscale. Geophysical Research Letters, 2016, 43, 5988-5996.	4.0	10
144	Reconstruction of Extreme Geomagnetic Storms: Breaking the Data Paucity Curse. Space Weather, 2020, 18, e2020SW002561.	3.7	10

#	Article	IF	CITATIONS
145	Modeling the response of the induced magnetosphere of Venus to changing IMF direction using MESSENGER and Venus Express observations. Geophysical Research Letters, 2009, 36, .	4.0	9
146	Statistical Relations Between Fieldâ€Aligned Currents and Precipitating Electron Energy Flux. Geophysical Research Letters, 2018, 45, 8738-8745.	4.0	9
147	Iridium Communications Satellite Constellation Data for Study of Earth's Magnetic Field. Geochemistry, Geophysics, Geosystems, 2021, 22, e2020GC009515.	2.5	9
148	Storm Time Plasma Pressure Inferred From Multimission Measurements and Its Validation Using Van Allen Probes Particle Data. Space Weather, 2020, 18, e2020SW002583.	3.7	9
149	Characterization of 6-pentyl-?-pyrone from the soil fungusTrichoderma koningii. Die Naturwissenschaften, 1990, 77, 539-540.	1.6	8
150	Magnetosphere dynamics during the 14ÂNovember 2012 storm inferred from TWINS, AMPERE, Van Allen Probes, and BATS-R-US–CRCM. Annales Geophysicae, 2018, 36, 107-124.	1.6	8
151	The Magnetometer Instrument on MESSENGER. , 2007, , 417-450.		8
152	Dipolarization in the inner magnetosphere during a geomagnetic storm on 7 October 2015. Geophysical Research Letters, 2016, 43, 9397-9405.	4.0	7
153	Structure and Configuration of Mercury's Magnetosphere. , 2018, , 430-460.		7
154	Bifurcated Region 2 Fieldâ€Aligned Currents Associated With Substorms. Journal of Geophysical Research: Space Physics, 2020, 125, e2019JA027041.	2.4	7
155	On the relation between electric fields in the inner magnetosphere, ring current, auroral conductance, and plasmapause motion. Geophysical Monograph Series, 2005, , 159-166.	0.1	6
156	The double auroral oval in the duskâ€midnight sector: Formation, mapping and dynamics. Journal of Geophysical Research, 2012, 117, .	3.3	6
157	Current Closure in the Auroral Ionosphere: Results From the Auroral Current and Electrodynamics Structure Rocket Mission. Geophysical Monograph Series, 2013, , 183-192.	0.1	6
158	New Insights into the Substorm Initiation Sequence from the Spatioâ€ŧemporal Development of Auroral Electrojets. Journal of Geophysical Research: Space Physics, 0, , .	2.4	6
159	A comparison of smallâ€scale magnetic fluctuations in the Region 1 and 2 fieldâ€sligned current systems. Journal of Geophysical Research: Space Physics, 2017, 122, 3277-3290.	2.4	5
160	Statistical Study of Mercury's Energetic Electron Events as Observed by the Gammaâ€Ray and Neutron Spectrometer Instrument Onboard MESSENGER. Journal of Geophysical Research: Space Physics, 2018, 123, 4961-4978.	2.4	4
161	Upstream conditions at Mercury during the first MESSENGER flyby: Results from two independent solar wind models. Geophysical Research Letters, 2009, 36, .	4.0	3

162 MESSENGER: Exploring Mercury's Magnetosphere. , 2007, , 133-160.

3

#	Article	IF	CITATIONS
163	The Magnetic Field of Mercury. Space Sciences Series of ISSI, 2009, , 307-339.	0.0	2
164	Science Goals and Mission Concept for a Landed Investigation of Mercury. Planetary Science Journal, 2022, 3, 68.	3.6	2
165	Statistical Analysis of Bifurcating Region 2 Field-Aligned Currents Using AMPERE. Frontiers in Astronomy and Space Sciences, 2022, 9, .	2.8	2
166	Reply to comment on "Empirical relationship between electron precipitation and farâ€ultraviolet auroral emissions from DMSP observations― Journal of Geophysical Research: Space Physics, 2013, 118, 6827-6828.	2.4	1
167	Introduction to the special issue of Icarus on "Mercury after Two MESSENGER Flybys― Icarus, 2010, 209, 1-2.	2.5	0
168	Observations of upstream ultra-low-frequency waves in the Mercury's foreshock. , 2014, , .		0
169	Overview of Solar Wind–Magnetosphere–lonosphere–Atmosphere Coupling and the Generation of Magnetospheric Currents. Space Sciences Series of ISSI, 2018, , 555-581.	0.0	0